

Parametric study of *E. coli* incidence with reference to the New Zealand freshwater standards and the Manawatū–Whanganui region

Stephen R Marsland¹, Robert I McLachlan², and Christopher Tuffley²

¹ School of Mathematics and Statistics, Victoria University of Wellington, New Zealand

² School of Fundamental Sciences, Massey University, New Zealand

Abstract

The New Zealand National Policy Statement for Freshwater Management 2020 sets several targets for freshwater quality, six of which are measurements of rivers; others relate to lakes. Each regional council is required to monitor freshwater quality and to respond as prescribed in order to meet the targets. One target of particular public interest is based on four criteria determined from recent *E. coli* readings, and concerns the health risk of swimming in a river. However, the inherent variability of the data makes it difficult to determine the water quality state and trend reliably, particularly using traditional methods based on percentiles. Therefore, in this study we return to the parametric lognormal model of *E. coli* distribution, from which the official criteria were developed. We interpret the classification system in terms of the parametric model and show that the parametric model can reduce uncertainty and can incorporate more useful information, especially from very high *E. coli* readings, and is suitable for censored data. We apply the parametric model for state and trend to 135 sites in the Manawatū–Whanganui region.

1 Introduction

In August 2017, the New Zealand Government approved amendments to the National Policy Statement (NPS) for Freshwater Management—the ‘Clean Water’ package. These amendments, in particular the criteria for a river to be deemed ‘swimmable’, had been the subject of extensive background research and were also of great public interest. Their adoption followed a period of some decades of refinements. Historical, public health, international comparison, and statistical and freshwater science issues related to the NPS are discussed by McBride [8]. The subject continues to be of national importance, as each regional council in New Zealand seeks to implement the NPS and to manage its freshwater monitoring and improvement programme. A new NPS, finalising the criteria, came into force on 3 September 2020 [9].

The swimmability criteria place rivers into 5 categories (A–E, also called Blue, Green, Yellow, Orange, and Red, of which A, B, and C are deemed ‘swimmable’), based on four

E. coli criteria, shown in Table 1¹

Two of the four criteria are based on percentiles (P50 and P95, i.e., the 50th and 95th percentiles of the *E. coli* counts), and two are based on ‘percentage exceedances’: G260 and G540 refer to the percentage of samples that should not exceed bacteria counts of 260 and 540, respectively. There is a further classification for sites that are likely to be used for swimming, based solely on 95% thresholds. In practice this classifies B, C, D, and E sites as Poor, and subdivides A sites into Excellent, Good, and Fair. We call the standard method based on P50, P95, G260, and G540 the *percentile classification*.

Regional councils are responsible for measuring and reporting against all targets. The data is generally collected monthly, from a set of pre-defined locations across the river systems of the region. These locations may be chosen for a variety of reasons, including upstream and downstream points close to potential polluters, convenience of sampling, and proximity to human settlements. New measurement points may be added if pollution is detected in a particular place.

Escherichia coli (*E. coli*) are bacteria found in the digestive tract of warm-blooded animals, some of which can cause sickness in humans. *E. coli* readings in freshwater, usually given as the number of bacteria present in a 100 mL sample, are highly variable. *E. coli* generally gets into rivers from human sewage outlets or from farm run-off. It then flows downstream. If its presence in the river is because of a contamination episode such as heavy rain or other adverse weather event, it will be present in the river system for only a few days, but if it comes from a persistent polluter it will be present continuously. Usually, monthly readings are essentially uncorrelated in time. A widely-used approach models *E. coli* readings as independent and lognormally-distributed random variables. For example, Sørensen *et al.* [12] use the lognormal parametric model to develop a sampling protocol for swimmability.

Moreover, *E. coli* concentrations are only a proxy for freshwater quality. The guidelines were developed by modelling the risk of *Campylobacter* infection *using* the lognormal parametric model of *E. coli* (see, e.g., [9, p. 48].) The thresholds were determined from a combination of this risk, historical precedent, and international comparisons. Percentile criteria (and categories) were adopted for easier comprehension by the public and to be clear and simple for councils to measure and report. This process of turning a multidimensional state into discrete ordinal categories (sometimes called *dichotomization* or *ordinalization*) necessarily loses information; the ordinal data should almost never be used for subsequent statistical analysis [4]. In addition it should be remembered that the goal of this and any other clean water strategy is not the specific targets (e.g., a fraction of rivers by length to be ‘A’ quality by a certain date), but an improvement in the underlying multidimensional state. A further complication is that the water quality criteria are used for several different purposes, namely (i) determining the state of a particular site; (ii) determining the trend in state of a particular site; (iii) determining a broad measure of the state or trend of all measured sites; (iv) predicting the state or trend of all rivers in the region.

The Manawatū–Whanganui Regional Council commissioned reports into the state and trend of regional rivers, and these were used to develop swimmability targets for 2030 and 2040 [11]. These studies examined each *E. coli* threshold separately, and the importance

¹The cabinet paper clarifies that “all four measures must be met and should be determined using a minimum of 60 samples over a maximum of five years collected on a regular basis regardless of weather and flow conditions. The only exception to this is if there is insufficient monitoring data to establish the 95th percentile, in which case that measure/statistic does not apply.”

Category	G540 samples above 540	P50 median	P95 95th percentile	G260 samples above 260
A — Blue	< 5%	≤ 130	≤ 540	< 20%
B — Green	5–10%	≤ 130	≤ 1000	20–34%
C — Yellow	10–20%	≤ 130	≤ 1200	20–34%
D — Orange	20–30%	> 130	> 1200	$> 34\%$
E — Red	$> 30\%$	> 260	> 1200	$> 50\%$

Table 1: *E. coli* criteria in the National Policy Statement for freshwater. Categories A, B, and C meet the national bottom line, informally known as ‘swimmable’. The NPS states that ‘Attribute state must be determined by satisfying all numeric attribute states’. (Presumably it is intended that a site with, for example, G540 <5%, median <130, and G260 =22% falls into category B.)

of sampling errors figure prominently. Notably, the 95th percentile criterion (P95) was discarded because it is estimated with lower precision than the other three criteria P50, G260, and G540. Trends in G260 and G540 were estimated from the trends in their annual values, which lowers their precision.

In this paper we compare the parametric lognormal model to the percentile classification and show that the parametric model can reduce uncertainty and can incorporate more useful information, especially from very high *E. coli* readings, and is suitable for censored data. We apply the parametric model for state and trend to 135 sites in the Manawatū–Whanganui region and make recommendations for points that are worth further consideration in the analysis of swimmability.

2 State determination in the parametric model

2.1 Interpretation of the NPS criteria in the parametric model

For state estimation, we consider a river in a steady state whose *E. coli* measurements at times t_i are independent random variables drawn from a lognormal distribution, i.e.:

$$L_i := \log(E. coli(t_i)) \in N(\mu, \sigma).$$

Here \log is the natural logarithm.

The water quality criteria have a simple interpretation in terms of this parametric model. Each individual criterion corresponds to a half-plane in the (μ, σ) parameter space, with each category A–E being an intersection of such half-planes, which corresponds to a polygon in (μ, σ) parameter space.

For example, the criterion that the median be less than or equal to 130 becomes the half-plane $\mu \leq \log(130) \approx 4.868$, and the criterion that 95th percentile is less than or equal to 1200 becomes the half-plane $\mu + z_{0.95}\sigma \leq \log(1200) \approx 7.0890$. Here z_p is the z -value corresponding to the quantile p for the normal distribution, i.e., the inverse of the cumulative density function. From Table 1, the relevant values are $z_{0.5} = 0$, $z_{0.66} = 0.412$, $z_{0.7} = 0.524$, $z_{0.8} = 0.842$, $z_{0.9} = 1.282$, and $z_{0.95} = 1.645$.

The individual criteria are shown in terms of the parametric model in Figure 1, and the resulting boundaries of these polygons for swimmability categories A–E in Figure 2. We summarize them as follows:

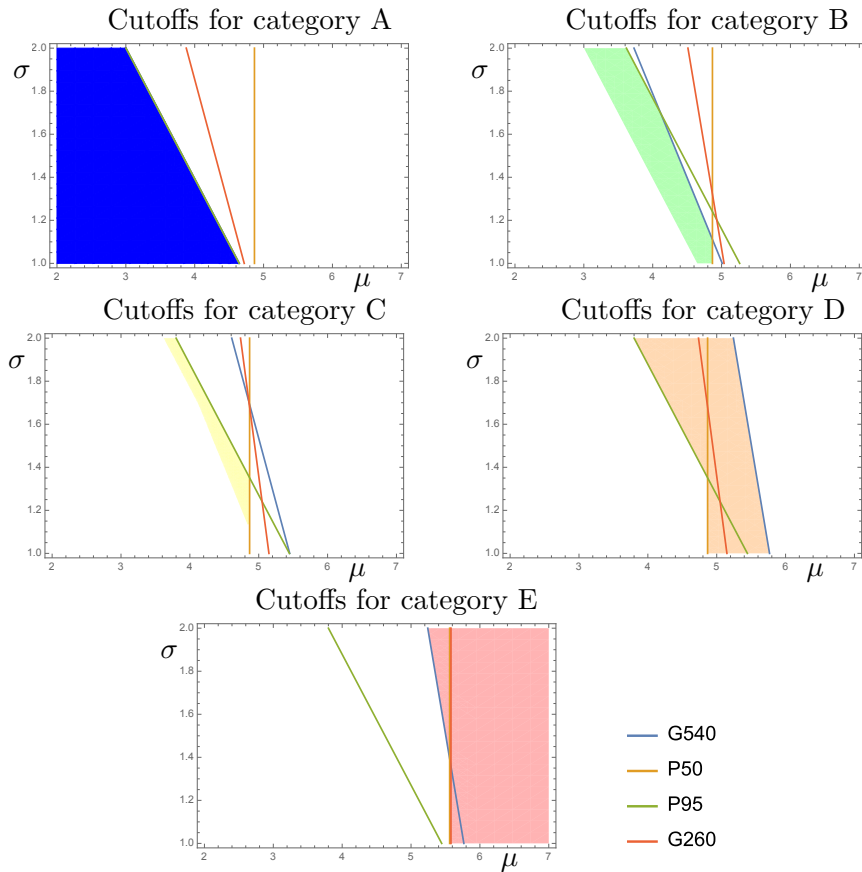


Figure 1: In the parametric model, each of the four swimmability criteria for each of the five categories corresponds to a half-plane in the (μ, σ) parameter space. For parameter values observed in practice, many of these criteria are inactive. Except for the D–E boundary, overall the P50 and P95 criteria are the most important.

A–B For the A–B boundary, only the P95 criterion (identical to G540 in this case) is relevant. All sites meeting P95 already greatly exceed the requirements for P50 and G260.

B–C The B–C boundary is determined for most sites by the G540 criterion. (For very clean sites P95 becomes active, and there is also a B–D boundary that is relevant for dirty sites, determined by P50, although in our data no sites came near either of these two parts of the boundary.) As G540 here is determined by the percentage of samples being above or below 10%, this is essentially equivalent to the 90th percentile.

C–D The C–D boundary—perhaps the most important, as it determines swimmability—is determined by P95 and P50. Sites meeting these criteria already satisfy G260 and G540.

D–E The D–E boundary is determined by G540, in this case equivalent to the 70th percentile.

Thus, the four criteria are not equally important for all sites.

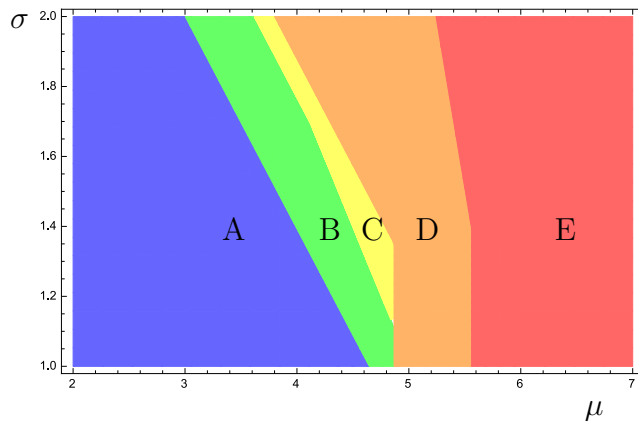


Figure 2: The five swimmability categories visualized in (μ, σ) parameter space in the parametric model.

Remarks

1. G260 and G540, on which a lot of attention has been placed, are likely to be irrelevant for determining whether a particular site is swimmable.
2. The criteria have the effect of making the category C region relatively small. For the sample data, far more sites are in category B than category C, which diminishes the usefulness of the categories. In terms of this model, it would make more sense to replace the B–C boundary at $P95 = 800$ instead of $P95 = 1000$.
3. The crucial C–D (pass–fail) boundary is mostly determined by $P95$. But $P95$ is the least reliable of the four criteria to measure, and is often dropped.
4. Dropping the 95th percentile requirement for the D–E boundary in favour of G540 requirement does make sense in this model.

2.2 Sampling errors in the parametric and percentile models

When n samples are drawn from a normal distribution with mean μ and standard deviation σ , the sampling error in the mean is σ/\sqrt{n} , and the sampling error in the standard deviation is $\sigma/\sqrt{2n}$. Therefore, the sampling error in $\mu + z_p\sigma$, the natural estimate of the p th percentile under the normal distribution, is $d_p\sigma/\sqrt{n}$ where $d_p = \sqrt{1 + \frac{1}{2}z_p^2}$.

There are different methods of estimating percentiles from data. In *E. coli* studies, this is often done by applying the Hazen method to the log of the bacteria counts [6], which is implemented in software provided by the Ministry for the Environment [8].

Sampling errors in percentiles are larger than sampling errors in $\mu + z_p\sigma$, as was pointed out in a study based on simulations [6]. The precise statement is that the sampling error in the p th percentile for a distribution with probability density function f and cumulative density function F is $c_p\sigma/\sqrt{n}$ where $c_p = \sqrt{p(1-p)}/f(F^{-1}(p))$ [13]. For example, the sampling error in the median for a normally-distributed random variable is $\sqrt{\frac{\pi}{2}}/\sqrt{n}$, a factor of 1.253 times larger than the sample error in the mean: see Figure 3 for an illustration of the differences as they affect the swimmability categories. Comparisons for different percentiles are given in Table 2.

The above values are approximations that are valid in the limit of large n . For small n , the bias of these estimators may be significant as well. The 50th percentile estimators

p	c_p	d_p	sampling factor
0.5	1.253	1	1.570
0.66	1.293	1.042	1.540
0.7	1.318	1.067	1.526
0.8	1.429	1.163	1.510
0.9	1.709	1.350	1.603
0.95	2.113	1.534	1.897

Table 2: Coefficients of the standard error in the $(100p)$ th percentile of data in $N(\mu, \sigma)$ in the limit of large n , as calculated by the percentile method (standard error $c_p\sigma/\sqrt{n}$) and from the parametric method (standard error $d_p\sigma/\sqrt{n}$), together with the ratio between the number of samples required by the percentile and parametric methods for the same sample error (so for the 95th percentile, the percentile method needs $(2.113/1.534)^2 = 1.897$ times as many samples to achieve the same sampling errors).

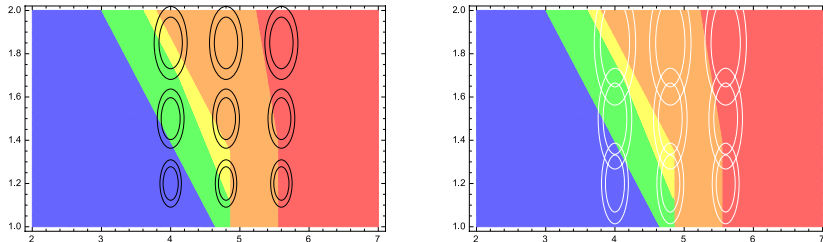


Figure 3: An illustration of 67% (1-sigma) confidence intervals when estimating the state of a single site with either 60 (large ellipses) or 120 (small ellipses) independent samples. Left: using the estimates of (μ, σ) from the parametric model. Right: Using percentiles in the parametric model leads to larger confidence intervals and larger sampling errors.

(the median and mean, respectively) are unbiased. The Hazen percentiles are biased: for example, for normal data the 95th percentile has bias -0.07σ when $n = 12$ and -0.008σ when $n = 60$. In contrast, the sample mean \bar{x} and sample standard deviation s easily provide the unbiased estimator $\bar{x} + \alpha sz_p$, where $\alpha = \sqrt{\frac{n-1}{2}} \Gamma(\frac{n-1}{2}) / \Gamma(\frac{n}{2})$ [10].

An example is shown in Figure 4 for synthetic data generated for a site with mean *E. coli* count of 150 and P95 count of 1750. With 60 independent samples, the percentile method falsely reports $P95 < 1200$ 18% of the time; in contrast, the parametric method falsely reports $P95 < 1200$ only 10% of the time.

2.3 *E. coli* data for the Manawatū–Whanganui region

Data were obtained from LAWA [7] for 135 sites in Manawatū–Whanganui. The 18,567 measurements ranged from January 2005 to December 2019. The number of observations per site ranged from 15 (there were 4 sites with fewer than 60 data points) to 189, with a median of 145 (i.e., 12 years of monthly sampling data). Observations are generally monthly with some missing observations.

A plot of all the data points for all 135 sites is shown in Figure 5. Changes in the measurement (or reporting) system over time can be seen, particularly with regard to precision and censoring (that is, reporting only a range in which the value lies). The reported precision varies with both time and value. Prior to 2008, mid-range values (near

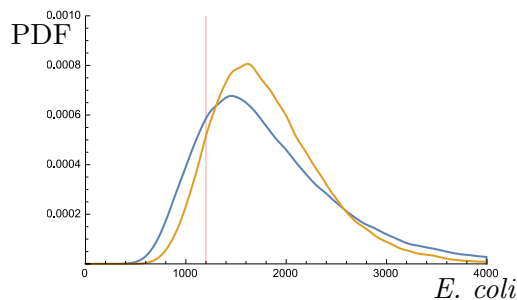


Figure 4: The distribution of estimates of the *E. coli* 95th percentile obtained by the parametric (orange) and percentile (blue) methods for synthetic data corresponding to a D-category site with median *E. coli* count of 150 and 95th percentile count of 1750. With 60 independent samples, the two methods falsely report P95<1200 18% (percentile) and 10% (parametric) of the time.

400) were rounded to the nearest 5 units (i.e., a precision of 1%); values less than 60 were rounded to the nearest 10 units; large values were reported as 9,800, 13,000, 14,100, 17,300, 19,900, 24,200, or 51,700. Some readings were censored, i.e., reported as ‘<10’ or ‘>24,200’.

From 2008 to mid-2012, there was no rounding, and the only censoring involved values reported as ‘<1’ (presumably because no bacteria were observed in the 100 mL sample). However, from mid-2012, values up to 2300 were reported to 2 significant figures, and higher values with gradually decreasing precision. High values for most sites were reported as 6,200, 6,900, 7,900, and 9,700. Low values were censored and reported as ‘<4’. Most high values were censored and reported as ‘>9,700’, although some sites continued to report higher values (up to 120,000, and ‘>240,000’).

Rounding is presumably related in some way to the underlying accuracy of the measurements; analytic errors in *E. coli* measurement are typically around 20% [2]. However, the rounding itself adds errors of 10–20%, especially for low and high values that are reported with less precision (consider values near 130, the critical threshold for P50). It may be unavoidable, but the question of whether it is necessary to add extra errors by rounding deserves a closer look. In this study we ignore the effect of rounding and analytic errors.

Censoring is more important. For example, the value ‘>9,700’ occurs 7 times for site 113, all of them since 2015, whereas the previous maximum reading was 3,683. These high *E. coli* counts are important to understanding the underlying state and trend of the river. Changing them to 9,700 would bias downwards the estimates of the mean, the standard deviation, and the trend. The value 9,700 is often only 1 standard deviation above the mean; 12 of the 135 sites have 95th percentile values over 9,700.

We deal with the censored values in the parametric model with a simple, standard approach in which censored values are replaced by their expected values in the model, conditioned on their known ranges. As the parameters now enter into both the model and the data, they obey nonlinear equations. We solve these by an iterative procedure in which the imputed values of the censored data values are iteratively updated. (Of course, the procedure becomes unreliable if too high a proportion of the data is censored.)

In an earlier study [11], censored values were removed from the data set before analysing trends. Since they tend to occur later in time, removing them biases trends downwards. The effect can be noticeable. For site 124, in which 3 of 51 values were

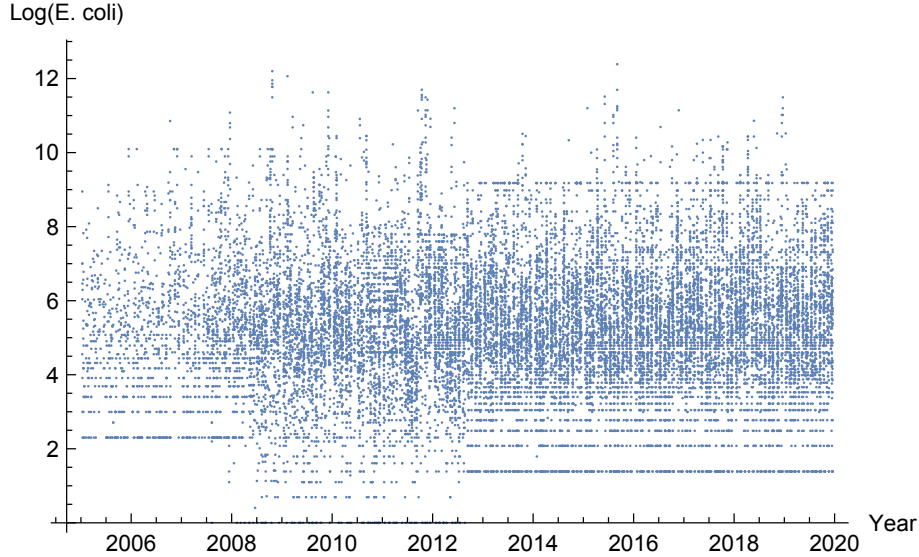


Figure 5: The 18,567 measurements of *E. coli* from 135 sites.

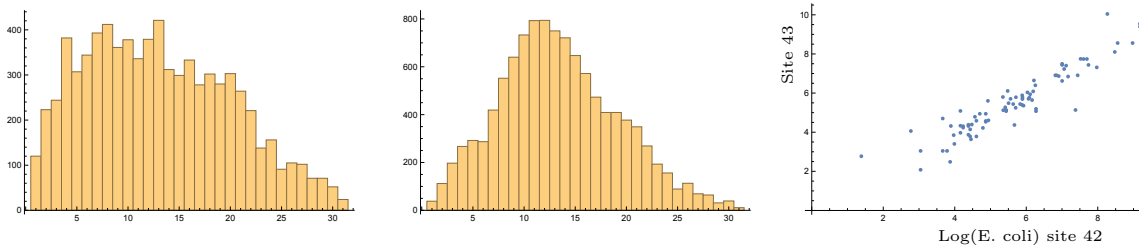


Figure 6: Histograms of day of the month for data collection. Left: prior to 2013; centre: from 2013. Right: scatterplot of all same-day readings from nearby sites 42 and 43, showing a correlation coefficient of 0.93.

censored, deleting the censored values gives a trend of -0.012 (i.e. 1.2% improvement per year) and a median *E. coli* count in 2020 of 209; replacing censored values with their bounds gives a trend of $+0.077$ and a median *E. coli* count in 2020 of 360; using imputed values gives a trend of $+0.103$ and a median *E. coli* count in 2020 of 421.

Collecting and analysing the water samples is time-consuming and expensive. A version of the data on LAWA that was available in 2018, but is no longer available, also listed the time of collection, which showed that nearby sites are sampled very nearly at the same time. This makes them correlated. We find that 434 pairs of sites have at least 30 measurements taken on the same day, with correlation between the same-day measurements greater than 0.5. The most highly correlated sites are 42 and 43, two sites on the Manawatū river in Palmerston North, less than 3 km apart. Their correlation coefficient is 0.93 (see Figure 6), which means that the data cannot be pooled to reduce uncertainty in the trend. Sample collection takes place mostly in the middle of the month (Fig. 6), even more so from 2013, which increases the chances of same-day collection, even between distant sites. The correlation may be due to an underlying cause, such as *E. coli* outbreaks linked to the same source, or rainfall triggering outbreaks.

Results for freshwater state using the parametric model are shown in Figure 8 and Tables 3 and 4. There are 24 ‘clean’ sites (categories A–C) and 111 ‘dirty’ sites (categories D–E) with no significant systematic difference between the percentile and parametric models.

3 Trends in the parametric model

The lognormal parametric model is convenient for trend determination. We first performed linear regressions to the data (t_i, L_i) for each site. The standard deviations of the residuals in the first half and in the second half of each site were compared. Over the set of all sites, the differences were not significant. Therefore we adopted the model $L_i \sim N(\mu + mt_i, \sigma)$, where the parameter m is the trend, and σ is the standard deviation of the residuals. A value of $m = -0.05$ means a 5% reduction in *E. coli* levels per year. In this model, the trends in all percentiles are equal, although the G260, P50, P95, and G540 criteria could be crossed at different times. The measured trends and their standard errors are shown in Figure 7.

The state A–E at time t is then determined from the parameters $(\mu + mt, \sigma)$. Note that σ is the standard deviation of the residuals and is smaller than the standard deviation of the data, as used for state determination. The standard errors of the parameters are also obtained. We report these at time 2020.

The results are shown in Table 3 (numbers of sites in each category in 2020); Figure 9 (a visualisation of the impact of 10-year trends on the 2020 category); Figures 10–12 (each data set plotted separately along with its trend); and Table 4 (numerical state and trend results for each site).

Of the 135 sites, 17 sites are improving at the 1-sigma level, 9 at least at the 2-sigma level, and 6 at the 3-sigma level. 18 sites are deteriorating at least at the 1-sigma level, 13 at least at the 2-sigma level, and 5 at the 3-sigma level. At 67 sites (50%) the trend was not significant at the 1-sigma level. The average trend is indistinguishable from 0.

However, each measured trend is subject to a sampling error. These have a median value of 0.034. This has the effect of smearing out the distribution of observed trends. (If all true trends were equal, we would observe a normal distribution of trends with standard deviation 0.053.) If the true trends are normally distributed with variance σ_1^2 and the sampling errors are independent and normally distributed with mean 0 and variance σ_2^2 , then the observed trends will be normally distributed with variance $\sigma_1^2 + \sigma_2^2$. Under these assumptions, the true distribution of trends is likely to be more concentrated than shown in the figure. However, the correlation between measurements at nearby sites makes it difficult to take this observation further.

Trends that are significant at less than the 1-sigma level should be treated with caution. (Sites with *any* improving trend have been called ‘more likely to be improving than not’ [11].) Site 47, Manawatū at Teacher’s College, showed a quite strong improving trend of about -0.15 (i.e. 15% per year) with $z_m \approx 1.3$ consistently from early 2013 to mid 2017. This was then reversed by several particularly high readings of up to 23,000. It is now showing a deteriorating trend of $+0.04$ with $z_m = 1.0$. It is not possible to determine from the data whether the water quality was actually improving until mid-2017 or whether this was just an artefact of noise, as the pattern seen here is typical of independent random samples.

How many samples are needed to detect a trend? For data drawn from the (μ, σ) model with n uniformly-spaced samples per year for T years, the expected standard error of the trend is $\sqrt{12}\sigma T^{-3/2}n^{-1/2}$ [1]. Adopting the (very minimal) requirement that to detect a trend m requires the expected standard error to be less than $|m|$, we need $n > \frac{12\sigma^2}{T^3 m^2}$.

Consider a site with a typical value of $\sigma = 1.5$. With 10 years of data and 12 samples

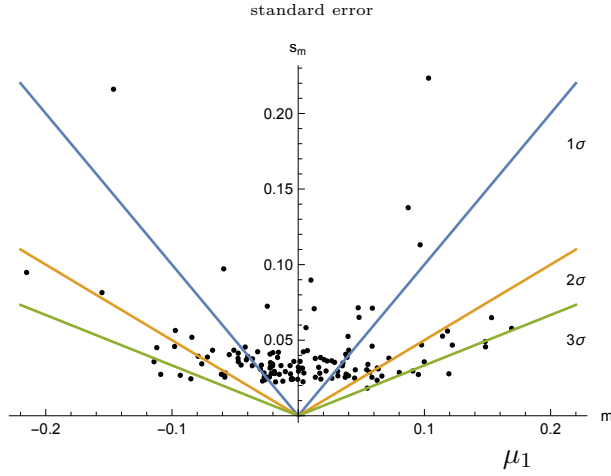


Figure 7: Scatterplot of trends for the 135 sites vs. standard error of each trend measurement. Regions in which an individual trend is significant at the 1, 2, and 3σ level are indicated. These sampling errors have the effect of smearing out the distribution of measured trends.

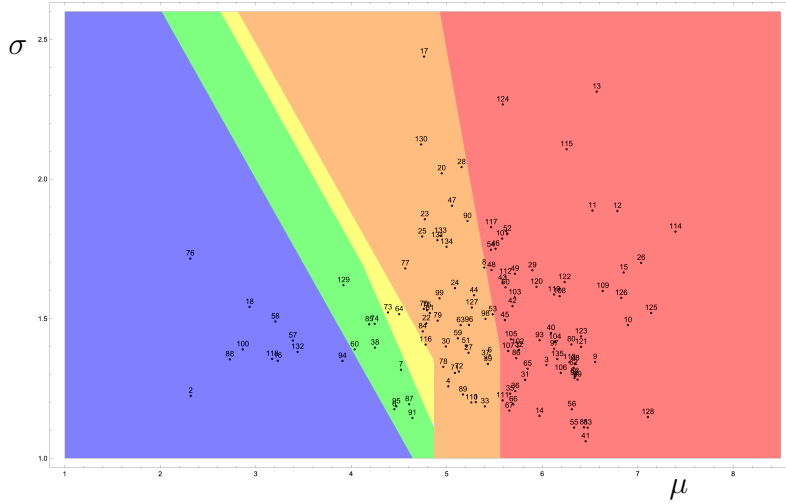


Figure 8: Results of the parametric model showing freshwater state (μ, σ) estimated using all data for each site.

per year, trends $|m| > 0.047$ are detectable; with 52 samples per year, trends $|m| > 0.023$ are detectable.

However, with 5 years of data and 12 samples per year, trends $|m| > 0.13$ are detectable; with 52 samples per year, trends $|m| > 0.064$ are detectable. In our dataset, only 5 of the 135 sites had $m < -0.13$ (sites 9, 17, 19, 26, 29) and some of these are exceptional (e.g., site 17, significant at $z = 11$ due to the installation of a new water treatment plant, and site 19 due to highly acidic water in the Whangaehu river, as shown in site 21 at which scarcely any *E. coli* are ever detected.)

Conversely, a number of sites have trends in the range -0.07 to -0.10 —good enough to move from the grade D/E boundary to the C/D boundary in 10 years. To detect this in 5 years even at the 1σ level needs weekly monitoring.

We conclude that to get useful trends in 5 years requires more frequent measurements than is the current practice.

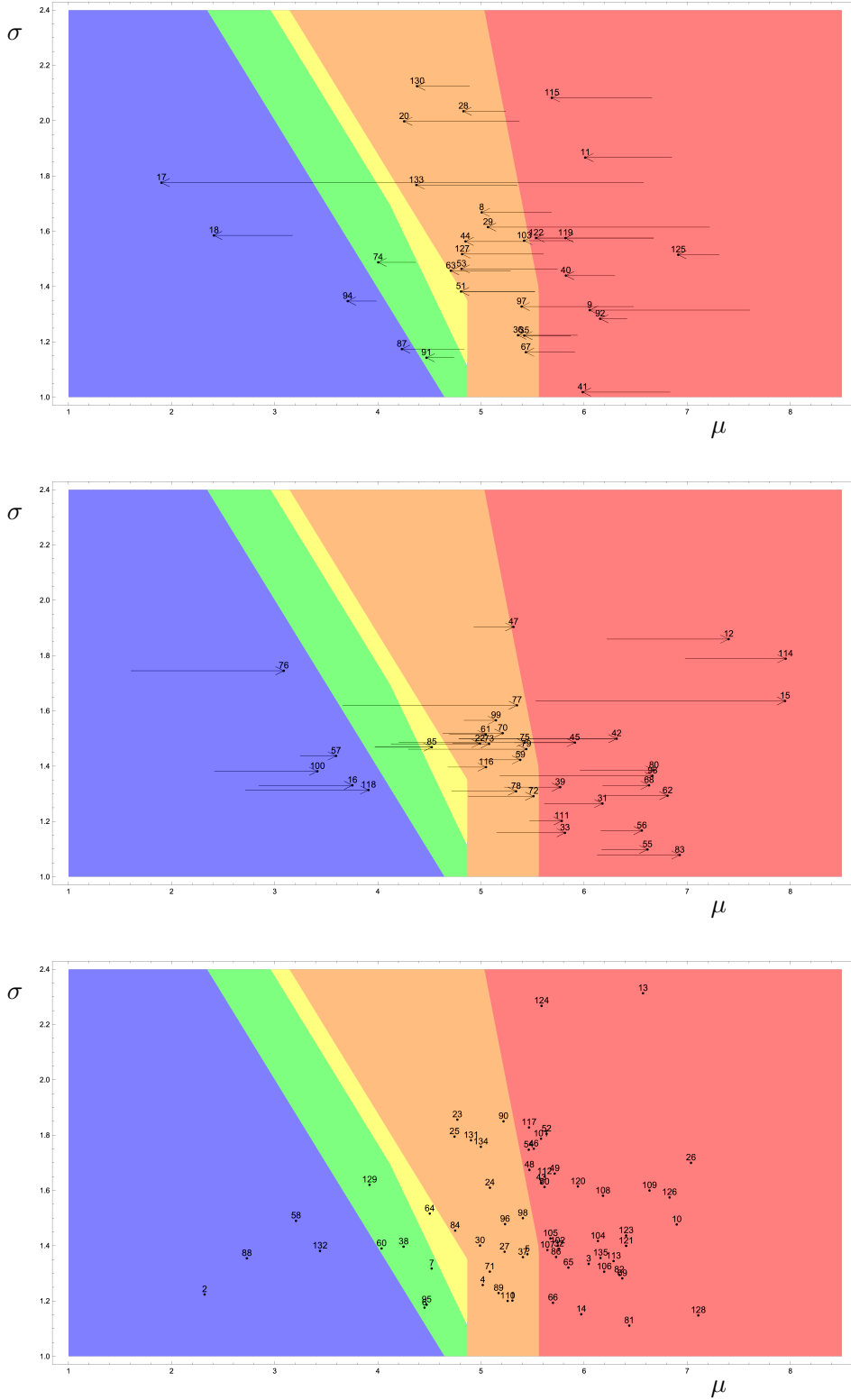


Figure 9: Results of the parametric model for trends. Top: Sites where the trend for freshwater quality is improving at the 1σ level, with an arrow pointing from the state estimated in 2010 to the state estimated in 2020. Middle: Sites where the trend for freshwater quality is deteriorating at the 1σ level. Bottom: Sites where the trend is not significant at the 1σ level, showing the average state. Note that many of the significant 10-year trends are of the same order as the sizes of the categories.

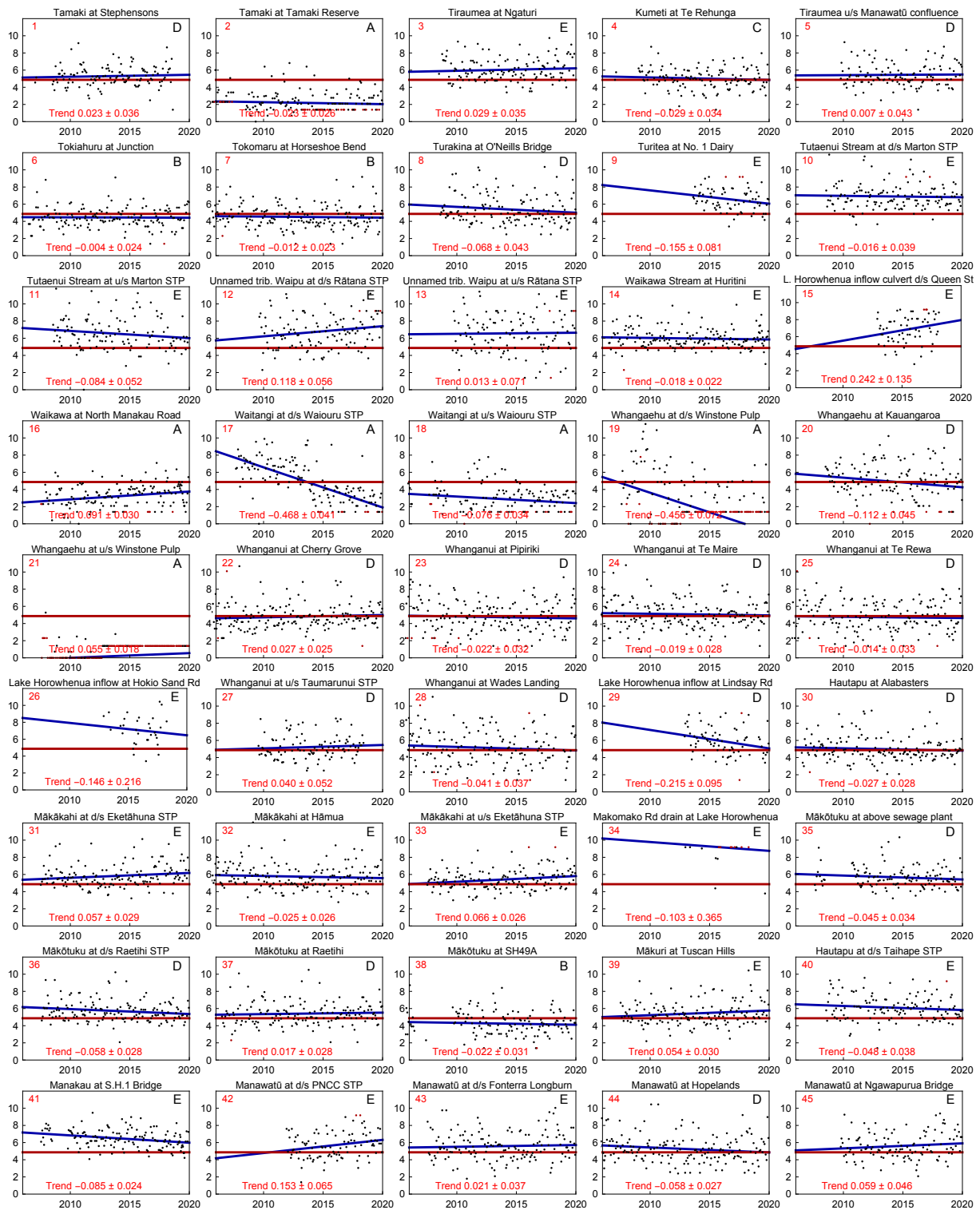


Figure 10: Log *E. coli* measurements and trends for sites 1–45. The red and blue lines show the P50 criterion and its trend, respectively. The trend, its standard error, and category in 2020 estimated from the trend are also shown. Censored data (for which imputed values are used) are shown in red.

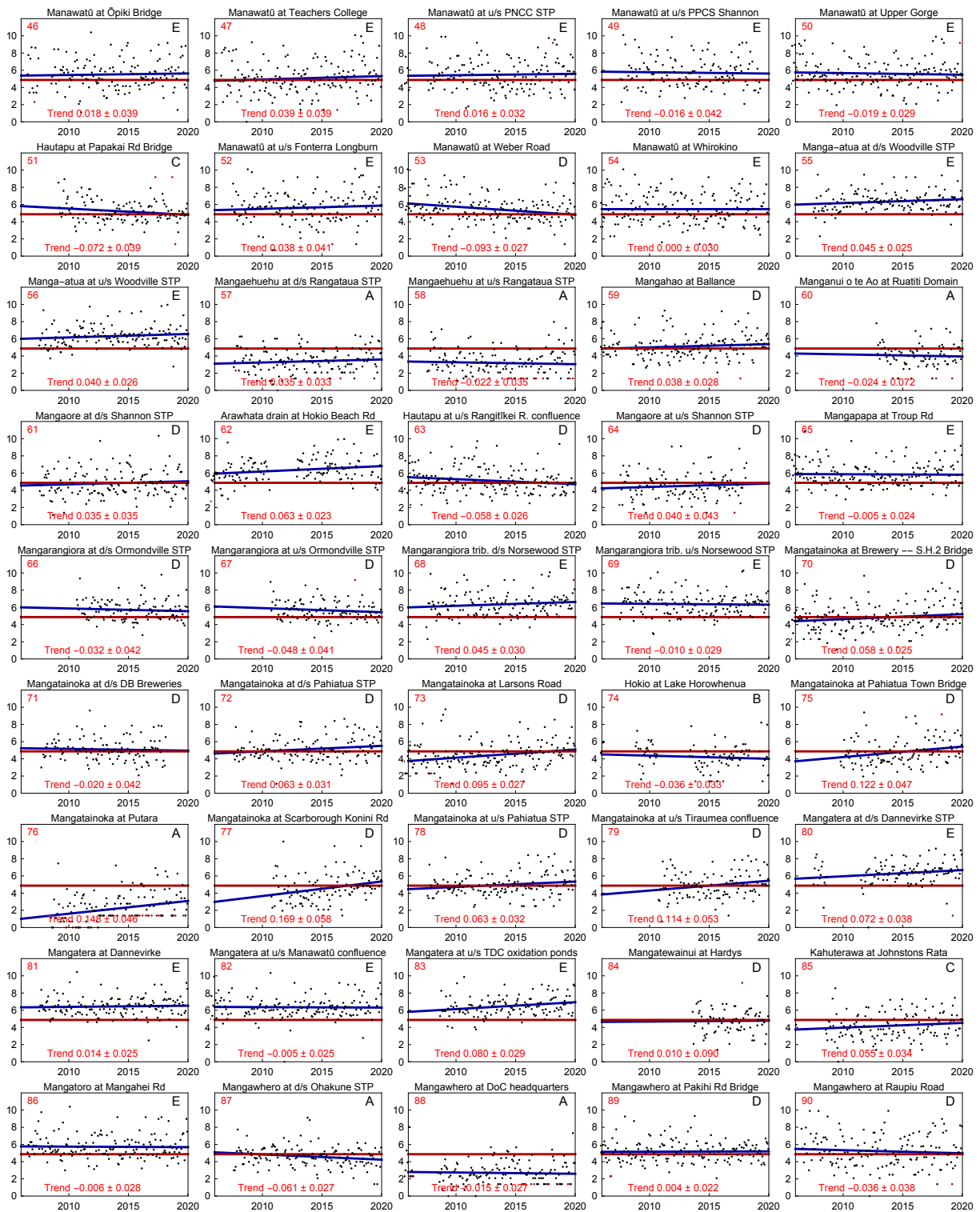


Figure 11: Log *E. coli* measurements and trends for sites 46–90. The red and blue lines show the P50 criterion and its trend, respectively. The trend, its standard error, and category in 2020 estimated from the trend are also shown. Censored data (for which imputed values are used) are shown in red.

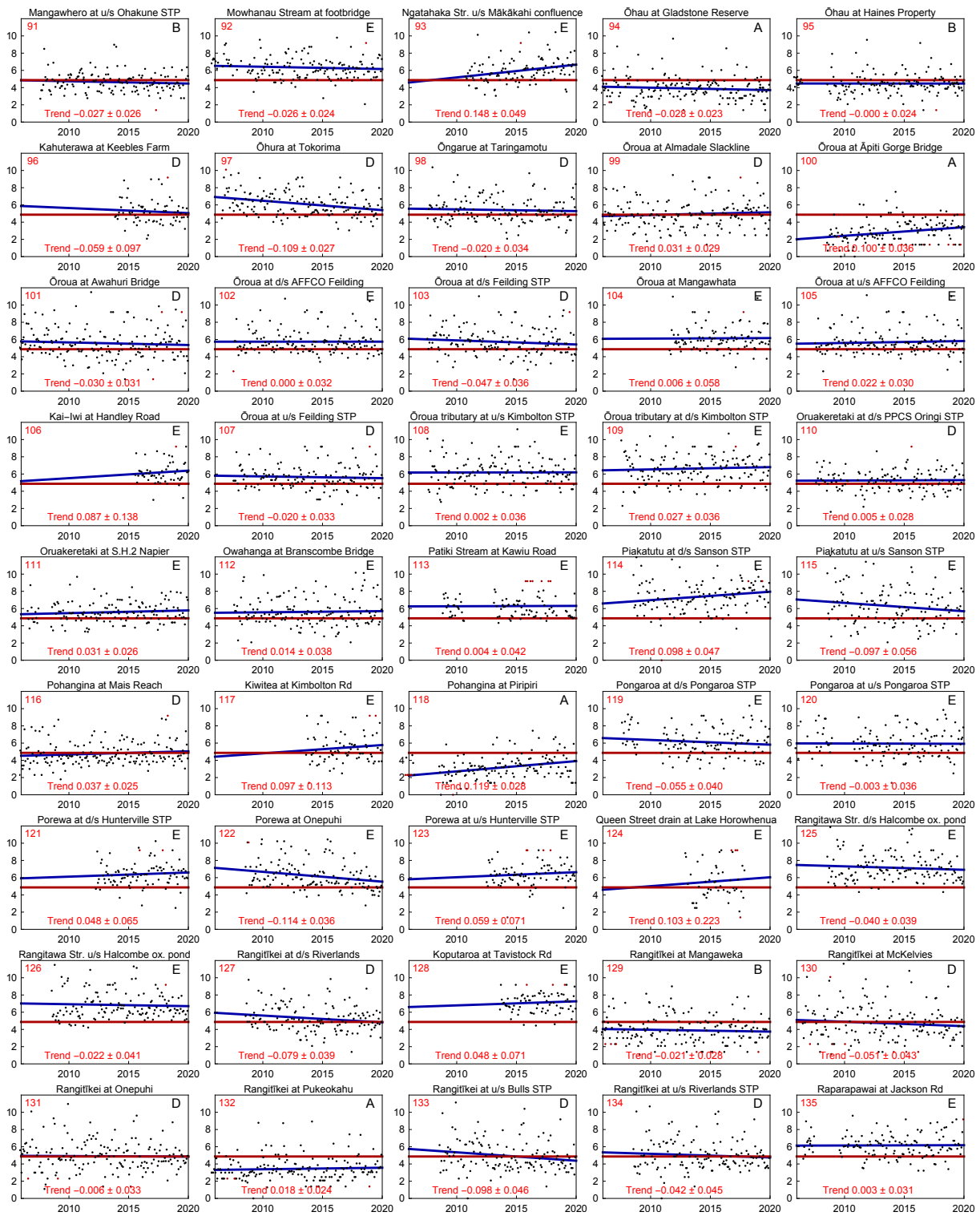


Figure 12: Log *E. coli* measurements and trends for sites 91–135. The red and blue lines show the P50 criterion and its trend, respectively. The trend, its standard error, and category in 2020 estimated from the trend are also shown. Censored data (for which imputed values are used) are shown in red.

	A	B	C	D	E
Percentile state	12	8	2	60	53
Average state	12	10	2	44	67
2020 state	16	7	3	44	61

Table 3: Number of Manawatū-Whanganui sites in each water quality category determined in two ways. Top row: Standard method, based on percentiles. Middle: from the parametric model, determining the average state using all data at each site. Bottom: From the parametric model, estimating the state in January 2020 using the fitted trend.

4 Discussion

Observations

1. Looking at the data in Figure 8, the classification system based on four different criteria of two different types (percentiles and percentage exceedances) seems to be unnecessarily complex. Very similar classifications, having a very similar relationship to health risks, can be obtained by a single criterion based on a single percentile. The 67% percentile is easier to measure reliably than the 95%, and would classify the data just as well. It would also allow the river state to be summarized by the single number $\mu + z_{0.67}\sigma$, which also retains more information than a classification into five classes.
2. This is backed up by Hunter [6], who concluded, “the estimation of the 95th percentile using any of the methods examined here offers little advantage over the current percentage exceedance approach, other than offering a false sense of increased accuracy. . . It is concluded that a move to use of 95th percentile calculations in determining compliance with bathing water standards has no statistical validity and has a number of disadvantages.”
3. The definition of category C means that very few sites fall into category C. Changing the category boundaries so that more nearly equal number of sites fall into categories B and C would have allowed the categorisation system to convey more information.
4. The system used in LAWA [7] for reporting states and trends is not transparent. For example, nearly all sites in the region are reported as showing either an improving or a deteriorating trend. Most likely, many of these are not significant. In the parametric model, only 24% of the trends are significant at the 2σ level, not accounting for multiple testing or correlation between sites.
5. We have not tested the validity of the lognormal model in detail. 95% of the residuals have $|z| < 2$ (consistent with the normal distribution) but 1.2% have $z < -2$ and 4% have $z > 2$ (cf. 2.2% in the normal distribution). The discrepancy in $2 < z < 3$ could repay further examination.

Recommendations

1. Examine why the data was rounded and if possible, avoid rounding.
2. Examine why the data was truncated and if possible, avoid truncation (censoring). These processes may be losing useful information for no good reason.
3. If possible, use an *E. coli* analysis method sensitive down to 1 bacteria/100 ml.
4. Faster, more reliable detection of trends needs more frequent sampling. It is more cost-effective to sample more frequently from fewer sites, as sampling nearby sites at the same time yields almost no independent information.
5. Re-examine the criteria used for reporting water quality states and trends. In particular, the 95% criterion is the deciding factor for swimmability for many sites, and should be examined carefully.

Acknowledgements This project arose from a problem presented by Horizons Regional Council (HRC) at the 2018 meeting of the Mathematics in Industry Study Group of New Zealand. We thank HRC (particularly Stacey Binsted, Abby Matthews and Manas Chakraborty) for their advice and the other members of the working group (including Ali Abdul Adheem, Jamas Enright, Anton Good, Christian Offen, Cami Sawyer, Sunchai Tongsuksai, Alex White, and Matt Wilkins) who examined various aspects of freshwater quality monitoring in the Horizons region.

References

- [1] S Ahn and J A Fessler (2003). Standard errors of mean, variance, and standard deviation estimators. EECS Department, The University of Michigan, 1-2.
- [2] D E Angelescu, V Huynh, A Hausot, G Yalkin, V Plet, J M Mouchel, S Guérin-Rechdaoui, S Azimi, V Rocher, Autonomous system for rapid field quantification of *Escherichia coli* in surface waters, *J. Appl. Microbiology* **126** (2019), 332–343.J
- [3] S Chatterjee and D L McLeish, Fitting linear regression models to censored data by least squares and maximum likelihood methods, *Commun. Stat. Th. Meth.* **15** (1986): 3227–3243.
- [4] V Fedorov, F Mannino, and R Zhang, Consequences of dichotomization, *Pharm. Stat.* **8** (1) (2009), 50-61.
- [5] C Fraser and T Snelder, State and Trends of River Water Quality in the Manawatū–Whanganui Region, Horizons Report 2018/EXT/1619, November 2018
- [6] P R Hunter, Does calculation of the 95th percentile of microbiological results offer any advantage over percentage exceedence in determining compliance with bathing water quality standards?, *Lett. Appl. Microbiology* **34** (2002), 283–286.
- [7] LAWA (Land Air Water Aotearoa), <http://lawa.org.nz>, accessed December 2020.
- [8] G McBride, National Objectives Framework: Statistical considerations for design and assessment, NIWA, September 2016.

- [9] Ministry for the Environment, National Policy Statement for Freshwater Management 2020, Publication ME 1518, 2020. Available online at <https://www.mfe.govt.nz/publications/fresh-water/national-policy-statement-freshwater-management-2020>
- [10] R S Parrish, Comparison of quantile estimators in normal sampling, *Biometrics* **46** 1990, 247–257.
- [11] T Snelder, Assessment of recent reductions in *E. coli* and sediment in rivers of the Manawatū–Whanganui Region, LWP Client Report 2017-06, January 2018.
- [12] P S Sørensen, J La Cour Jansen, and H Spliid, Statistical control of hygienic quality of bathing water, *Environmental Monitoring and Assessment* **17** (1991), 217–226.
- [13] A Stuart and K Ord, *Kendall's Advanced Theory of Statistics, Volume 1, Distribution Theory*, 6th ed., Wiley 2010.

i	Name of site i	N_i	Cat ₁	μ	s_μ	σ	Cat ₂	m	z_m	μ_{2020}	$s_{\mu_{2020}}$	σ_{2020}	Cat ₃
1	Tamaki at Stephensons	121	D	5.31	0.11	1.20	D	0.02	0.63	5.45	0.26	1.20	D
2	Tamaki at Tamaki Reserve	160	A	2.32	0.10	1.22	A	-0.02	0.89	2.04	0.21	1.34	A
3	Tiraumea at Ngaturi	135	E	6.05	0.11	1.33	E	0.03	0.82	6.21	0.23	1.33	E
4	Kumeti at Te Rehunga	132	D	5.02	0.11	1.26	D	-0.03	0.87	4.86	0.22	1.25	C
5	Tiraumea u/s Manawatū confluence	119	D	5.45	0.13	1.37	D	0.01	0.17	5.49	0.26	1.37	D
6	Tokiahuru at Junction	157	B	4.45	0.09	1.18	B	0.00	0.17	4.42	0.19	1.18	B
7	Tokomaru at Horseshoe Bend	175	B	4.52	0.10	1.32	B	-0.01	0.53	4.43	0.20	1.32	B
8	Turakina at ONeills Bridge	137	D	5.39	0.14	1.68	D	-0.07	1.57	5.01	0.29	1.67	D ↑
9	Turitea at No. 1 Dairy	76	E	6.55	0.15	1.35	E	-0.16	1.91	6.05	0.30	1.31	E ↑
10	Tutaenui Stream at d/s Marton STP	136	E	6.90	0.13	1.48	E	-0.02	0.42	6.81	0.25	1.48	E
11	Tutaenui Stream at u/s Marton STP	119	E	6.53	0.17	1.89	E	-0.08	1.62	6.01	0.36	1.87	E ↑
12	Unnamed tributary of Waipu at d/s Rātana STP	124	E	6.79	0.17	1.89	E	0.12	2.11	7.40	0.33	1.86	E ↓
13	Unnamed tributary of Waipu at u/s Rātana STP	118	E	6.57	0.21	2.31	E	0.01	0.18	6.64	0.43	2.32	E
14	Waikawa Stream at Huritini	168	E	5.97	0.09	1.15	E	-0.02	0.80	5.86	0.17	1.15	E
15	Lake Horowhenua inflow at culvert d/s Queen St	64	E	6.85	0.21	1.67	E	0.24	1.79	7.95	0.64	1.64	E ↓
16	Waikawa at North Manakau Road	154	A	3.23	0.11	1.35	A	0.09	3.07	3.75	0.21	1.33	A ↓
17	Waitangi at d/s Waiouru STP	145	E	4.76	0.20	2.44	D	-0.47	11.33	1.90	0.29	1.78	A ↑
18	Waitangi at u/s Waiouru STP	141	A	2.94	0.13	1.54	A	-0.08	2.22	2.41	0.25	1.58	A ↑
19	Whangaehu at d/s Winstone Pulp	149	D	2.44	0.25	3.08	D	-0.46	6.31	-0.94	0.52	3.16	A ↑
20	Whangaehu at Kauangaroa	142	D	4.95	0.17	2.02	D	-0.11	2.49	4.26	0.32	2.00	D ↑
21	Whangaehu at u/s Winstone Pulp	145	A	0.90	0.07	0.81	A	0.05	3.00	0.55	0.13	0.78	A ↓
22	Whanganui at Cherry Grove	183	D	4.79	0.11	1.48	D	0.03	1.08	4.99	0.22	1.48	D
23	Whanganui at Pipiriki	177	D	4.77	0.14	1.86	D	-0.02	0.68	4.60	0.28	1.87	D
24	Whanganui at Te Maire	178	D	5.09	0.12	1.61	D	-0.02	0.67	4.95	0.24	1.61	D
25	Whanganui at Te Rewa	167	D	4.74	0.14	1.79	D	-0.01	0.41	4.64	0.28	1.80	D
26	Lake Horowhenua inflow at Hokio Sand Rd	32	E	7.04	0.30	1.70	E	-0.15	0.68	6.46	0.90	1.69	E
27	Whanganui at u/s Taumarunui STP	104	D	5.23	0.14	1.38	D	0.04	0.75	5.47	0.34	1.37	D
28	Whanganui at Wades Landing	160	E	5.16	0.16	2.04	D	-0.04	1.11	4.83	0.33	2.03	D

Table 4: Results of the linear parametric model. See last page for the key to the column headings.

i	Name of site i	N_i	Cat ₁	μ	s_μ	σ	Cat ₂	m	z_m	μ_{2020}	$s_{\mu_{2020}}$	σ_{2020}	Cat ₃
29	Lake Horowhenua inflow at Lindsay Rd	75	E	5.90	0.19	1.67	E	-0.22	2.27	5.07	0.41	1.61	D ↑
30	Hautapu at Alabasters	162	D	4.99	0.11	1.40	D	-0.03	0.96	4.81	0.22	1.40	D
31	Mākākahi at d/s Eketāhuna STP	149	E	5.82	0.10	1.28	E	0.06	1.97	6.18	0.21	1.26	E ↓
32	Mākākahi at Hāmua	172	D	5.76	0.11	1.39	E	-0.02	0.97	5.58	0.22	1.38	E
33	Mākākahi at u/s Eketāhuna STP	150	D	5.40	0.10	1.19	D	0.07	2.52	5.82	0.19	1.16	E ↓
34	Makomako Rd drain at Lake Horowhenua	15	E	8.73	0.53	2.04	E	-0.10	0.28	8.75	1.53	2.35	E
35	Mākōtuku at above sewage plant	123	D	5.66	0.11	1.23	E	-0.05	1.35	5.42	0.21	1.22	D
36	Mākōtuku at d/s Raetihi STP	148	D	5.72	0.10	1.24	E	-0.06	2.04	5.36	0.20	1.22	D ↑
37	Mākōtuku at Raetihi	156	D	5.41	0.11	1.36	D	0.02	0.61	5.52	0.22	1.36	D
38	Mākōtuku at SH49A	134	B	4.25	0.12	1.40	B	-0.02	0.71	4.11	0.23	1.40	B
39	Mākuri at Tuscan Hills	148	D	5.43	0.11	1.34	D	0.05	1.78	5.77	0.22	1.32	E ↓
40	Hautapu at d/s Taihape STP	130	E	6.09	0.13	1.45	E	-0.05	1.26	5.82	0.25	1.44	E
41	Manakau at S.H.1 Bridge	142	E	6.46	0.09	1.06	E	-0.09	3.48	5.99	0.16	1.02	E ↑
42	Manawatū at d/s PNCC STP	97	E	5.69	0.16	1.55	E	0.15	2.36	6.32	0.31	1.50	E ↓
43	Manawatū at d/s Fonterra Longburn	148	D	5.59	0.13	1.63	E	0.02	0.55	5.71	0.27	1.63	E
44	Manawatū at Hopelands	178	D	5.29	0.12	1.58	D	-0.06	2.16	4.85	0.23	1.56	D ↑
45	Manawatū at Ngawapurua Bridge	120	E	5.61	0.14	1.50	E	0.06	1.27	5.91	0.27	1.49	E ↓
46	Manawatū at Ōpiki Bridge	148	D	5.51	0.14	1.75	E	0.02	0.46	5.62	0.28	1.75	E
47	Manawatū at Teachers College	161	D	5.06	0.15	1.90	D	0.04	1.00	5.32	0.30	1.90	E
48	Manawatū at u/s PNCC STP	161	D	5.47	0.13	1.67	E	0.02	0.51	5.58	0.26	1.67	E
49	Manawatū at u/s PPCS Shannon	138	E	5.72	0.14	1.66	E	-0.02	0.37	5.61	0.31	1.66	E
50	Manawatū at Upper Gorge	172	D	5.62	0.12	1.61	E	-0.02	0.64	5.48	0.25	1.61	E
51	Hautapu at Papakai Rd Bridge	130	D	5.20	0.12	1.40	D	-0.07	1.85	4.81	0.24	1.38	C ↑
52	Manawatū at u/s Fonterra Longburn	148	E	5.64	0.15	1.80	E	0.04	0.93	5.87	0.30	1.80	E
53	Manawatū at Weber Road	170	D	5.48	0.12	1.52	D	-0.09	3.49	4.81	0.22	1.46	D ↑
54	Manawatū at Whirokino	182	E	5.46	0.13	1.75	E	0.00	0.01	5.47	0.26	1.75	E
55	Manga-atua at d/s Woodville STP	150	E	6.34	0.09	1.11	E	0.04	1.79	6.62	0.18	1.10	E
56	Manga-atua at u/s Woodville STP	150	E	6.31	0.10	1.18	E	0.04	1.51	6.56	0.19	1.17	E

Table 4: Results of the linear parametric model. See last page for the key to the column headings.

i	Name of site i	N_i	Cat ₁	μ	s_μ	σ	Cat ₂	m	z_m	μ_{2020}	$s_{\mu_{2020}}$	σ_{2020}	Cat ₃
57	Mangaehuehu at d/s Rangataua STP	148	A	3.39	0.12	1.42	A	0.03	1.06	3.59	0.24	1.44	A
58	Mangaehuehu at u/s Rangataua STP	148	A	3.21	0.12	1.49	A	-0.02	0.63	3.05	0.25	1.53	A
59	Mangahao at Ballance	160	D	5.12	0.11	1.43	D	0.04	1.38	5.38	0.22	1.42	D
60	Manganui o te Ao at Ruatiti Domain	86	B	4.04	0.15	1.39	B	-0.02	0.34	3.94	0.30	1.40	A
61	Mangaore at d/s Shannon STP	147	D	4.82	0.13	1.52	D	0.04	1.02	5.05	0.25	1.51	D
62	Arawhata drain at Hokio Beach Rd	146	E	6.33	0.11	1.32	E	0.06	2.66	6.81	0.21	1.29	E ↓
63	Hautapu at u/s Rangitikei River confluence	177	D	5.15	0.11	1.48	D	-0.06	2.28	4.71	0.22	1.46	D ↑
64	Mangaore at u/s Shannon STP	127	D	4.50	0.13	1.52	C	0.04	0.92	4.79	0.34	1.52	D
65	Mangapapa at Troup Rd	173	E	5.85	0.10	1.32	E	-0.01	0.23	5.81	0.20	1.32	E
66	Mangarangiora at d/s Ormondville STP	111	E	5.70	0.11	1.19	E	-0.03	0.76	5.55	0.23	1.19	D
67	Mangarangiora at u/s Ormondville STP	111	D	5.66	0.11	1.17	E	-0.05	1.15	5.44	0.22	1.16	D
68	Mangarangiora tributary at d/s Norsewood STP	146	E	6.35	0.11	1.34	E	0.05	1.49	6.63	0.22	1.33	E
69	Mangarangiora tributary at u/s Norsewood STP	150	E	6.37	0.10	1.28	E	-0.01	0.35	6.31	0.21	1.28	E
70	Mangatainoka at Brewery — S.H.2 Bridge	189	D	4.76	0.11	1.54	D	0.06	2.30	5.21	0.23	1.52	D ↓
71	Mangatainoka at d/s DB Breweries	114	D	5.09	0.12	1.31	D	-0.02	0.48	4.95	0.31	1.30	D
72	Mangatainoka at d/s Pahiatua STP	137	D	5.13	0.11	1.31	D	0.06	2.04	5.51	0.22	1.29	D ↓
73	Mangatainoka at Larsons Road	172	D	4.39	0.12	1.52	C	0.10	3.49	5.08	0.23	1.48	D ↓
74	Hokio at Lake Horowhenua	107	B	4.25	0.14	1.48	B	-0.04	1.10	4.00	0.26	1.49	B
75	Mangatainoka at Pahiatua Town Bridge	120	D	4.79	0.14	1.53	D	0.12	2.61	5.42	0.28	1.49	D ↓
76	Mangatainoka at Putara	136	A	2.32	0.15	1.72	A	0.15	3.25	3.09	0.31	1.74	A ↓
77	Mangatainoka at Scarborough Konini Rd	111	D	4.57	0.16	1.68	D	0.17	2.93	5.35	0.31	1.62	D ↓
78	Mangatainoka at u/s Pahiatua STP	139	D	4.97	0.11	1.33	D	0.06	1.98	5.34	0.22	1.31	D ↓
79	Mangatainoka at u/s Tiraumea confluence	110	D	4.91	0.14	1.49	D	0.11	2.17	5.44	0.28	1.46	D ↓
80	Mangatera at d/s Dannevirke STP	115	E	6.31	0.13	1.41	E	0.07	1.89	6.68	0.24	1.39	E ↓
81	Mangatera at Dannevirke	145	E	6.44	0.09	1.11	E	0.01	0.53	6.52	0.18	1.11	E
82	Mangatera at u/s Manawatū confluence	158	E	6.34	0.10	1.29	E	-0.01	0.22	6.30	0.21	1.29	E
83	Mangatera at u/s TDC oxidation ponds	134	E	6.48	0.10	1.11	E	0.08	2.80	6.93	0.19	1.08	E ↓
84	Mangatewainui at Hardys	77	C	4.75	0.17	1.45	D	0.01	0.11	4.78	0.33	1.45	D

Table 4: Results of the linear parametric model. See last page for the key to the column headings.

i	Name of site i	N_i	Cat ₁	μ	s_μ	σ	Cat ₂	m	z_m	μ_{2020}	$s_{\mu_{2020}}$	σ_{2020}	Cat ₃
85	Kahuterawa at Johnstons Rata	141	C	4.19	0.12	1.48	B	0.06	1.63	4.52	0.24	1.47	C ↓
86	Mangatoro at Mangahei Rd	159	D	5.73	0.11	1.36	E	-0.01	0.22	5.69	0.21	1.36	E
87	Mangawhero at d/s Ohakune STP	144	B	4.61	0.10	1.19	B	-0.06	2.22	4.23	0.20	1.17	A ↑
88	Mangawhero at DoC headquarters	153	A	2.73	0.11	1.35	A	-0.01	0.55	2.59	0.22	1.40	A
89	Mangawhero at Pakihi Rd Bridge	171	D	5.17	0.09	1.23	D	0.00	0.17	5.20	0.19	1.23	D
90	Mangawhero at Raupiu Road	159	D	5.22	0.15	1.85	D	-0.04	0.96	4.98	0.29	1.85	D
91	Mangawhero at u/s Ohakune STP	148	B	4.64	0.09	1.14	B	-0.03	1.05	4.47	0.19	1.14	B
92	Mowhanau Stream at footbridge	162	E	6.34	0.10	1.29	E	-0.03	1.10	6.16	0.19	1.28	E
93	Ngatahaka Stream u/s Mākākahi confluence	110	E	5.97	0.14	1.42	E	0.15	3.02	6.66	0.26	1.37	E ↓
94	Ōhau at Gladstone Reserve	181	A	3.91	0.10	1.35	A	-0.03	1.23	3.71	0.19	1.35	A
95	Ōhau at Haines Property	156	B	4.47	0.09	1.19	B	0.00	0.02	4.47	0.18	1.19	B
96	Kahuterawa at Keebles Farm	72	D	5.23	0.17	1.48	D	-0.06	0.61	5.05	0.35	1.47	D
97	Ōhura at Tokorima	158	E	6.13	0.11	1.39	E	-0.11	3.98	5.39	0.21	1.33	D ↑
98	Ōngarue at Taringamotu	146	D	5.41	0.12	1.50	D	-0.02	0.59	5.28	0.25	1.50	D
99	Ōroua at Almadale Slackline	169	D	4.93	0.12	1.57	D	0.03	1.06	5.15	0.24	1.57	D
100	Ōroua at Āpiti Gorge Bridge	137	A	2.86	0.12	1.39	A	0.10	2.80	3.41	0.24	1.38	A ↓
101	Ōroua at Awahuri Bridge	179	D	5.58	0.13	1.79	E	-0.03	0.97	5.36	0.27	1.78	D
102	Ōroua at d/s AFFCO Feilding	147	D	5.74	0.12	1.40	E	0.00	0.00	5.74	0.23	1.40	E
103	Ōroua at d/s Feilding STP	148	E	5.71	0.13	1.58	E	-0.05	1.33	5.42	0.26	1.57	D
104	Ōroua at Mangawhata	101	E	6.13	0.14	1.42	E	0.01	0.11	6.16	0.28	1.42	E
105	Ōroua at u/s AFFCO Feilding	153	D	5.67	0.12	1.43	E	0.02	0.75	5.82	0.22	1.42	E
106	Kai-Iwi at Handley Road	54	E	6.20	0.18	1.31	E	0.09	0.63	6.39	0.36	1.30	E
107	Ōroua at u/s Feilding STP	140	D	5.64	0.12	1.38	E	-0.02	0.61	5.52	0.24	1.38	D
108	Ōroua tributary at u/s Kimbolton STP	149	E	6.18	0.13	1.58	E	0.00	0.04	6.19	0.26	1.58	E
109	Ōroua tributary at d/s Kimbolton STP	149	E	6.63	0.13	1.60	E	0.03	0.73	6.80	0.26	1.60	E
110	Oruakeretaki at d/s PPCS Oringi STP	140	D	5.26	0.10	1.20	D	0.00	0.16	5.29	0.20	1.20	D
111	Oruakeretaki at S.H.2 Napier	148	D	5.59	0.10	1.21	E	0.03	1.19	5.78	0.19	1.20	E
112	Owahanga at Branscombe Bridge	147	D	5.62	0.14	1.65	E	0.01	0.36	5.70	0.27	1.65	E

Table 4: Results of the linear parametric model. See last page for the key to the column headings.

i	Name of site i	N_i	Cat ₁	μ	s_μ	σ	Cat ₂	m	z_m	μ_{2020}	$s_{\mu_{2020}}$	σ_{2020}	Cat ₃
113	Patiki Stream at Kawiu Road	96	E	6.29	0.14	1.34	E	0.00	0.10	6.31	0.26	1.35	E
114	Piakatutu at d/s Sanson STP	133	E	7.40	0.16	1.81	E	0.10	2.09	7.96	0.31	1.79	E ↓
115	Piakatutu at u/s Sanson STP	129	E	6.26	0.19	2.11	E	-0.10	1.73	5.69	0.38	2.08	E ↑
116	Pohangina at Mais Reach	172	D	4.78	0.11	1.41	D	0.04	1.46	5.05	0.21	1.40	D
117	Kiwitea at Kimbolton Rd	76	D	5.47	0.21	1.83	E	0.10	0.85	5.78	0.42	1.82	E
118	Pohangina at Piripiri	148	A	3.17	0.11	1.36	A	0.12	4.30	3.91	0.21	1.31	A ↓
119	Pongaroa at d/s Pongaroa STP	127	E	6.13	0.14	1.59	E	-0.05	1.35	5.82	0.27	1.58	E ↑
120	Pongaroa at u/s Pongaroa STP	135	E	5.94	0.14	1.61	E	0.00	0.10	5.92	0.26	1.61	E
121	Porewa at d/s Hunterville STP	93	E	6.41	0.15	1.40	E	0.05	0.74	6.60	0.29	1.40	E
122	Porewa at Onepuhi	142	E	6.24	0.14	1.63	E	-0.11	3.20	5.53	0.26	1.58	E ↑
123	Porewa at u/s Hunterville STP	87	E	6.41	0.15	1.44	E	0.06	0.83	6.64	0.31	1.43	E
124	Queen Street drain at Lake Horowhenua	51	E	5.59	0.32	2.27	E	0.10	0.46	6.04	1.04	2.25	E
125	Rangitawa Stream at d/s Halcombe ox. pond	137	E	7.14	0.13	1.52	E	-0.04	1.02	6.91	0.26	1.52	E
126	Rangitawa Stream at u/s Halcombe ox. pond	137	E	6.83	0.13	1.57	E	-0.02	0.55	6.70	0.27	1.57	E
127	Rangitikei at d/s Riverlands	136	D	5.26	0.13	1.54	D	-0.08	2.01	4.82	0.26	1.52	D ↑
128	Koputaroa at Tavistock Rd	77	E	7.11	0.13	1.15	E	0.05	0.67	7.26	0.26	1.15	E
129	Rangitikei at Mangaweka	182	D	3.92	0.12	1.62	B	-0.02	0.76	3.75	0.24	1.64	B
130	Rangitikei at McKelvies	160	D	4.73	0.17	2.12	D	-0.05	1.18	4.38	0.34	2.12	D ↑
131	Rangitikei at Onepuhi	169	D	4.90	0.14	1.78	D	-0.01	0.19	4.85	0.28	1.79	D
132	Rangitikei at Pukeokahu	179	A	3.44	0.10	1.38	A	0.02	0.74	3.56	0.21	1.40	A
133	Rangitikei at u/s Bulls STP	137	D	4.94	0.15	1.80	D	-0.10	2.14	4.37	0.30	1.77	D ↑
134	Rangitikei at u/s Riverlands STP	137	D	5.00	0.15	1.76	D	-0.04	0.92	4.76	0.30	1.75	D
135	Raparapawai at Jackson Rd	137	E	6.16	0.12	1.36	E	0.00	0.11	6.18	0.22	1.36	E

Table 4: Results of the percentile, parametric state, and parametric trend models. N_i : number of measurements at site i .

Cat₁: water quality category using all data and Hazen percentiles.

$(\mu, s_\mu, \sigma, \text{Cat}_2)$: mean (and its standard error), standard deviation, and category, all data, parametric state model.

$(m, z_m, \mu_{2020}, s_{\mu_{2020}}, \sigma_{2020}, \text{Cat}_3)$: trend and its z -score, mean (and its standard error), standard deviation, and category at 2020 in the linear trend model.

Sites that are improving (resp. deteriorating) by at least 0.05 (i.e., by at least 5% per year) at the 1-sigma level are marked ↑ (resp. ↓).

Macrons have been added to names as accurately as possible using the sources available to us. In cases of doubt, the name recorded in the New Zealand Geographic Board *Gazetteer* has been used.